

Geophysical Research Letters

RESEARCH LETTER

10.1029/2019GL082578

Key Points:

- Video footage shows tsunami inundation within 1-2 min after the mainshock with periods shorter than those recorded by the local tide gauge
- Published rupture models predict up to 5-m tsunami runups but cannot explain their timing, amplitude, and period as reconstructed from videos
- Videos reveal key role of suitably designed escape routes and vertical platforms for timely self-evacuation from rapid tsunami inundation

Supporting Information:

- · Supporting Information S1
- · Data Set S1

Correspondence to:

M. Carvajal, matias.carvajal.ramirez@gmail.com

Citation:

Carvajal, M., Araya-Cornejo, C., Sepúlveda, I., Melnick, D., & Haase, J. S. (2019). Nearly instantaneous tsunamis following the *Mw* 7.5 2018 Palu earthquake. *Geophysical Research Letters*, 46, 5117–5126. https://doi.org/ 10.1029/2019GL082578

Received 1 MAR 2019 Accepted 18 APR 2019 Accepted article online 24 APR 2019 Published online 16 MAY 2019

Nearly Instantaneous Tsunamis Following the *Mw* 7.5 2018 Palu Earthquake

Matías Carvajal^{1,2}, Cristian Araya-Cornejo³, Ignacio Sepúlveda⁴, Daniel Melnick^{2,5}, and Jennifer S. Haase⁴

¹Programa de Doctorado en Ciencias Geológicas, Facultad de Ciencias Químicas, Universidad de Concepción, Concepción, Chile, ²Millennium Nucleus The Seismic Cycle Along Subduction Zones, Valdivia, Chile, ³Observatorio en Gestión del Riesgo de Desastres, Universidad Bernardo O'Higgins, Santiago, Chile, ⁴Cecil H. and Ida M. Green Institute of Geophysics and Planetary Physics, Scripps Institution of Oceanography, University of California, San Diego, La Jolla, CA, USA, ⁵Instituto de Ciencias de la Tierra, Universidad Austral de Chile, Valdivia, Chile

Abstract The tsunami observations produced by the 2018 magnitude 7.5 Palu strike-slip earthquake challenged the traditional basis underlying tsunami hazard assessments and early warning systems. We analyzed an extraordinary collection of 38 amateur and closed circuit television videos to show that the Palu tsunamis devastated widely separated coastal areas around Palu Bay within a few minutes after the mainshock and included wave periods shorter than 100 s missed by the local tide station. Although rupture models based on teleseismic and geodetic data predict up to 5-m tsunami runups, they cannot explain the higher surveyed runups nor the tsunami waveforms reconstructed from video footage, suggesting either these underestimate actual seafloor deformation and/or that non-tectonic sources were involved. Post-tsunami coastline surveys combined with video evidence and modeled tsunami travel times suggest that submarine landslides contributed to tsunami generation. The video-based observations have broad implications for tsunami hazard assessments, early warning systems, and risk-reduction planning.

Plain Language Summary Tsunami hazard assessment is routinely based on assessing the impacts of long-period waves generated by vertical seafloor motions reaching the coast tens of minutes after the earthquake in typical subduction-zone environments. This view is inadequate for assessing hazard associated with strike-slip earthquakes such as the magnitude 7.5 2018 Palu earthquake, which resulted in tsunami effects much larger than would normally be associated with horizontal fault motion. From an extraordinary collection of 38 amateur and closed circuit television videos we estimated tsunami arrival times, amplitudes, and wave periods at different locations around Palu Bay, where the most damaging waves were reported. We found that the Palu tsunamis devastated widely separated coastal areas within a few minutes after the mainshock and included unusually short wave periods, which cannot be explained by the earthquake fault slip alone. Post-tsunami surveys show changes in the coastline, and this combined with video footage provides potential locations of submarine landslides as tsunami sources that would match the arrival times of the waves. Our results emphasize the importance of estimating tsunami hazards along coastlines bordering strike-slip fault systems and have broad implications for considering shorter-period nearly instantaneous tsunamis in hazard mitigation and tsunami early warning systems.

1. Introduction

Sulawesi Island in the central part of Indonesia is located in a complex tectonic setting where the Australian, Sunda, and Philippine plates meet in a triple junction (Socquet et al., 2006; Walpersdorf et al., 1998). This region is characterized by distributed deformation over a broad region, which can be explained by block rotations along active faults with variable kinematics. Earthquake and tsunami events have repeatedly affected this region in the recorded history (Katili, 1970). The most recent tsunami occurred on the evening of 28 September 2018, at 18:02:45, local time (UTC+8), when a moment magnitude (*Mw*) 7.5 earthquake ruptured a ~200-km-long segment of the Palu-Koro strike-slip fault, which bisects Sulawesi and connects with the Minahassa Trench in the north (Bellier et al., 2001; Socquet et al., 2006; Walpersdorf et al., 1998; Watkinson et al., 2012; Watkinson & Hall, 2017; Figure 1a). In this region, three tsunamigenic earthquakes were reported in the past century (1927, 1968, and 1996) with accompanying tsunamis of up to 10 m (Soloviev & Go, 1974), most of them presumably associated with vertical motions caused by either thrust or normal faulting (Prasetya et al., 2001). In contrast, the Palu earthquake was associated with horizontal

©2019. American Geophysical Union. All Rights Reserved.

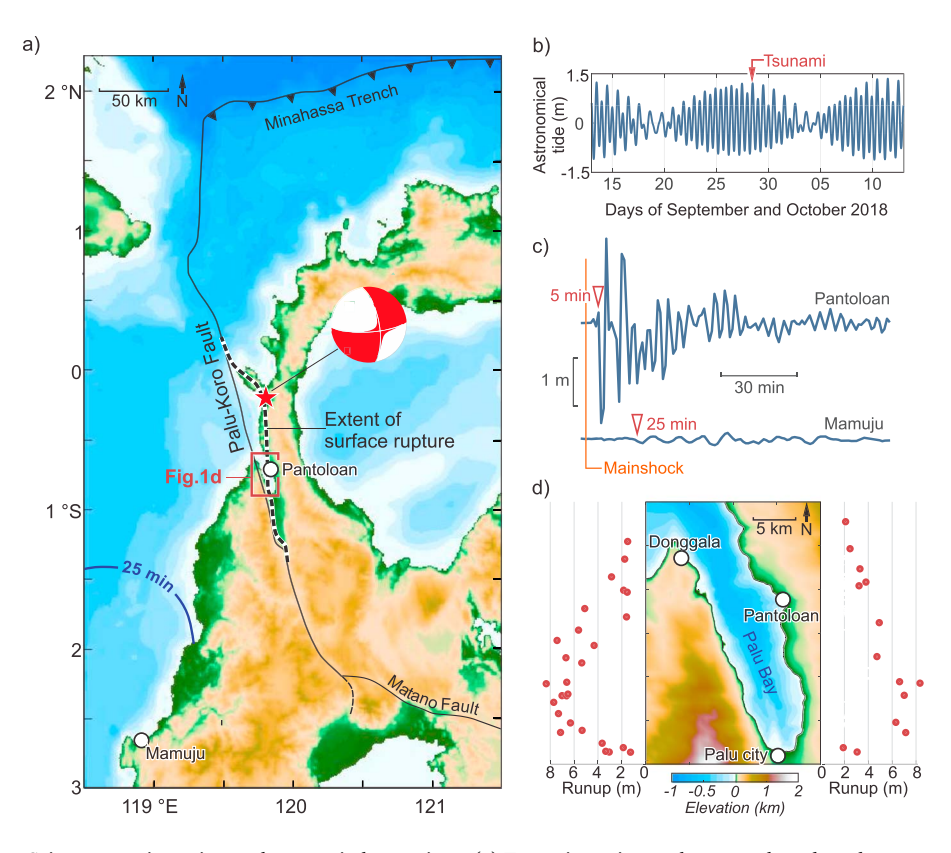


Figure 1. Seismotectonic setting and tsunami observations. (a) Tectonic setting and proposed earthquake rupture of the *Mw* 7.5 strike-slip Palu earthquake (Socquet et al., 2019). Black dashed line indicates the surface rupture proposed by Socquet et al. (2019); red star denotes the epicenter and focal mechanism from USGS (2018). Blue isoline indicates 25-min travel time for a point source tsunami originating at Mamuju. (b) Timing of the tsunami relative to 30 days of predicted astronomical tides for Palu Bay. Note that the tsunami occurred during a high tide of ~1 m above mean sea level. (c) De-tided records of the Palu tsunamis at Pantoloan and Mamuju. The arrival times of the first evident perturbations are indicated in reddish triangles. (d) Topobathymetric map of Palu Bay (Informasi Geospasial, 2018a) and surveyed tsunami runup heights (Fritz et al., 2018).

motion caused by strike-slip faulting. Rupture models based on distant teleseismic waveforms (U.S. Geological Survey, USGS, 2018) and onshore space geodesy data (Socquet et al., 2019) consistently indicate up to ~7 m of horizontal slip confined above 10-km depth with local dip-slip motion of up to only 2 m (Socquet et al., 2019).

Large tsunamis following the Palu earthquake rapidly attracted the attention of the scientific community. Although strike-slip earthquakes have caused historical (Imamura et al., 1995) and recent tsunamis (Hornbach et al., 2010), their amplitudes were much smaller than those observed around Palu Bay, where runups over 8 m were measured in field surveys (Figure 1d; Fritz et al., 2018; Muhari et al., 2018; Omira et al., 2019). This suggests that (i) despite its predominant strike-slip mechanism, the earthquake was capable of producing significant, coseismic vertical deformation beneath the bay, (ii) that tsunami waves were largely amplified by the unusual bathymetric features of the long and narrow bay (Figure 1d), and/or (iii) that additional non-tectonic sources contributed to tsunami generation. To gain insight into this problem, Heidarzadeh et al. (2019) compared tsunami waveforms predicted by numerical modeling with the two closest tide gauge records available for this event (Pantoloan and Mamuju, Figure 1c). They suggested that additional tsunami sources were required and that submarine landslides were the most reasonable candidates. However, these results were likely biased by the use of GEBCO bathymetry for tsunami modeling, which in some locations shows water depths 3 times smaller than those reported on higher-resolution charts (Informasi Geospasial, 2018a). Moreover, their analysis relied only on the Pantoloan tide gauge record (Figure 1c), which is relatively far (15 km) from the area affected by the largest waves (Figure 1d).

Here, we complement the Pantoloan tide gauge data with non-conventional evidence inferred from a novel approach that combines the analysis of video footage and satellite imagery. We used an extraordinary



collection of video images that captured different phases of the tsunami event (i.e., formation, propagation, and inundation) to derive quantitative estimates of their amplitudes, periods and timing around Palu Bay. Our analysis provides temporal data that is not possible to recover in field surveys (Fritz et al., 2018; Muhari et al., 2018; Omira et al., 2019). By tracking sea level changes from image pixels in subsequent frames, we constructed accurately timed tsunami waveforms from the quantitative interpretation of video footage (e.g., Fritz et al., 2006, 2012; Koshimura & Hayashi, 2012). In addition to providing valuable observations to constrain further source studies, we show that hazardous, short-period tsunamis struck nearly instantaneously with the seismic shaking at several locations around the bay and that these short-period waves were not recorded by the Pantoloan tide gauge station due to its longer sampling interval.

2. Video-Based Characterization of the Palu Tsunamis

Our extensive search on social media platforms resulted in 38 videos showing tsunami behavior at 14 sites around Palu Bay (white and magenta circles on Figure 2a; Table S1 and Data Set S1 in the supporting information), from which 23 provide relevant spatiotemporal information at six sites that can be used to reconstruct tsunami waveforms (Table S2 and Text S1). All videos were further used to support the satellite imagery analysis conducted to derive inundation distances around Palu Bay. We will refer to these videos by the names shown in Figure 2a and Table S1. The richness of tsunami information depends on the quantity and quality of the videos, which differ substantially among locations. While tsunamis at some places were observed by a single amateur video, others were precisely captured by several closed circuit television (CCTV) cameras.

In Figure 2b, the waveforms derived from video footage show the tsunami amplitude and timing at six locations (see Data Set S2 for waveform data). For reference we show the simulated tsunami waveforms predicted from the Socquet et al. (2019; blue) and USGS (2018; tan) earthquake rupture models. The tsunami occurred at high tide, corresponding to ~1 m above mean sea level (MSL). The vertical coseismic seafloor deformation generated by the source model at each location added to the tidal value gives the initial sea surface elevation above MSL shown in the figure. For example, at Dupa, the Socquet et al. (2019) model, which concentrates slip beneath the center of the bay, predicts negligible vertical coseismic deformation and therefore the initial value is nearly the tidal level (i.e., 1 m above MSL). On the other hand, the USGS (2018) model predicts significant coseismic subsidence of the seafloor at Dupa; therefore, the water drops with the land instantaneously in our simulations, producing an initial sea level of approximately 0.5 m above MSL. See Text S1 for the details of the waveform reconstruction procedure.

Probably the most remarkable features of the tsunamis that devastated Palu were the very short, nearly instantaneous arrival times. Usually, it is assumed that the time lag between an earthquake and its associated tsunami spans from tens of minutes to several hours (Cienfuegos et al., 2018; Mori et al., 2011), depending on the distance to the source region. However, CCTV footage from the Kampung Nelayan Hotel (KN Hotel), on the southeast coast of Palu Bay, recorded devastating tsunamis arriving 100 s after the seismic shaking (videos 1-6 and compiled video 42, Text S2, and Figure S1). This extremely short arrival time is robustly estimated by the difference in the timing between seismic shaking and water inundation using three cameras that had a clear view of the coastline (videos 1-3). Another array of CCTV cameras at Wani, located 20 km north of KN Hotel, showed tsunami inundation 3.5 min after the seismic shaking, which include the time needed for the tsunami to reach the site located 150 m inland (videos 7 and 8, Text S3, and Figure S2). If we assume a typical 5-m/s inundation rate, a positive-polarity wave (water level rise) should have reached the coast of Wani about 3 min after the mainshock (Figure 2b). Such an inference is consistent with reports from crewmembers of a passenger ship that was stranded on the adjacent coast (Figure S2 and video 9), who unanimously reported that immediately after the earthquake the sea level retreated significantly and was followed 3-5 min later by a large wave (Associated Press, 2018; Chicago Tribune, 2018; Text S3). This sea level pattern is consistent with the vertical movements of a container ship berthed at the Pantoloan port, 2.5 km south of Wani. There, a CCTV camera recorded more than ~2 m of water drawdown ~3 min after the end of seismic shaking followed by a rapid sea level rise of at least ~4 m (Figure 2b, video 11, Text S4, and Figure S3). In summary, videos collected at the KN Hotel, Wani, and Pantoloan (~20-km maximum separation) indicate rapid widespread tsunami inundation following the earthquake and provide valuable reconstructions of tsunami sea level waveforms at these locations (Figure 2b).

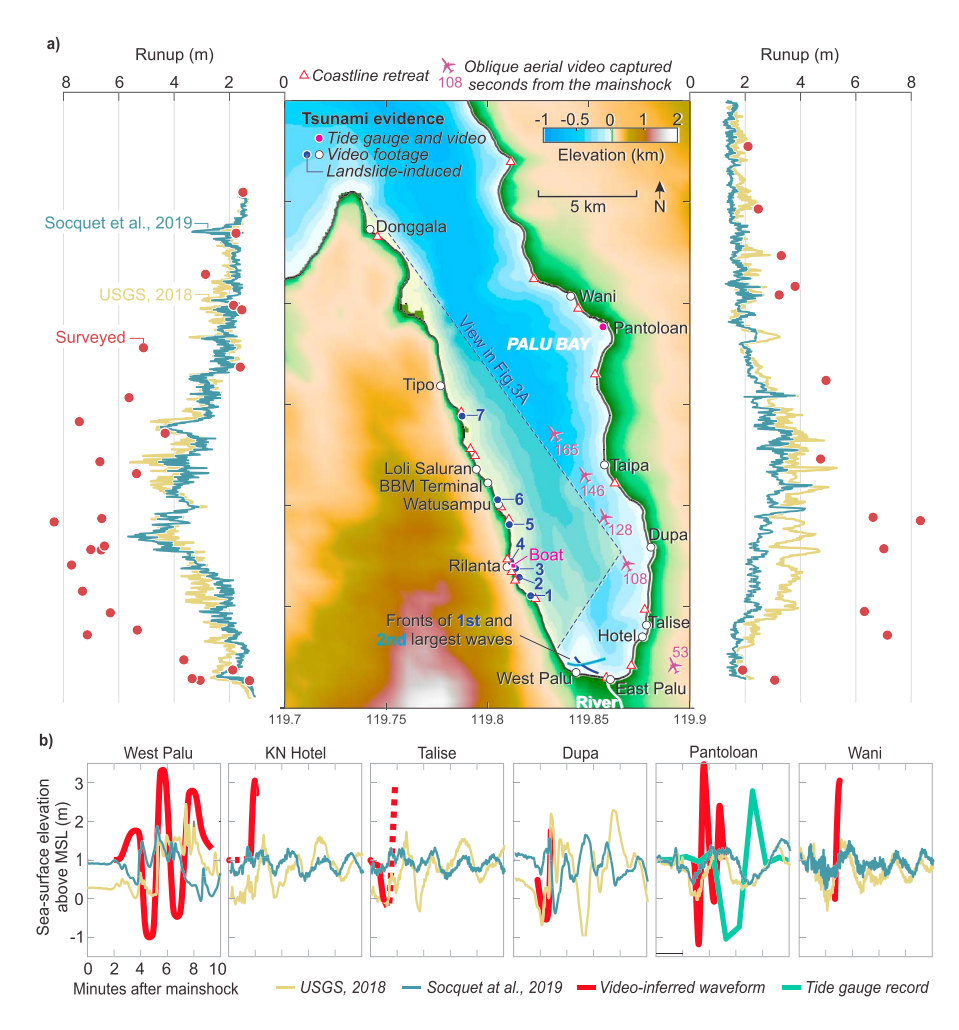


Figure 2. Observations and modeling results. (a) Map showing tsunami video location names (white and magenta circles), location of coastline retreat identified from satellite imagery (triangles), and flight path and timing (in seconds after the mainshock) of the aircraft pilot who recorded the point-source tsunamis shown in Figure 3a (video 38). The left and right panels show a comparison of tsunami runups measured by field surveys (Fritz et al., 2018) with those simulated based on existing coseismic slip models (Socquet et al., 2019; USGS, 2018). (b) Tsunami waveforms reconstructed from video footage (red) and predicted by the Socquet et al. (2019; blue) and USGS (2018; tan) coseismic slip models. The red dashed lines represent the waveform segments interpreted from videos with lower confidence (see text). Tsunami waveforms (available in Data Set S2) were inferred using videos 15–21 at Palu west (see video compilation 43), videos 1–3 at the KN Hotel (see video compilation 42), video 13 at Talise, video 14 at Dupa, video 11 at Pantoloan, and videos 7 and 8 at Wani (Table S2). Note the longer period waveform of the Pantoloan tide gauge record (green) with respect to the waveform reconstructed from closed circuit television footage (red). Tsunami simulations (runups in a and waveforms in b) and the video-inferred tsunami waveforms (b) are plotted as sea surface elevation including the high tide level of ~1 m above mean sea level at the time of the earthquake (Figure 1b).

Negative-polarity waves (water level drawdown) occurring immediately after the earthquake followed by tsunami inundation were observed at some sites but were not ubiquitous around the bay. For example, at Talise, an evident water retreat occurred almost instantaneously with seismic shaking (continuous red line in the Talise waveform of Figure 2b), which then appeared to be followed by a large wave that spurred people to run landward (dashed red line in the Talise waveform of Figure 2b; video 13). A very similar spatiotemporal behavior of sea level appeared to occur ~4 km north at Dupa, where a tsunami bore rapidly formed after an evident water drawdown (Figure 2b and video 14). However, negative-polarity leading waves followed by bore fronts, if existed, were not evident in the CCTV videos at the KN Hotel (see video 3), which is located 5 km south of Dupa and only 1 km from Talise. Instead, we infer an initial positive inundation from a rapid sea level increase of at least 2 m (Figure 2b and video 3).



Bore-type tsunamis followed by water retreat characterized the tsunamis that devastated the western parts of Palu city. Here, the tsunamis were captured by seven amateur videos collected within the Palu Grand Mall (videos 15-21 and compiled video 43 and Figure S4). The videos complement each other, in terms of view angles and temporal windows, and we were thus able to construct a quantitative composite estimate of arrival time, amplitudes and wave periods (Figure 2b). The video analysis shows that most of the destruction throughout Palu city was caused by two large tsunami waves arriving after smaller, but still significant, leading waves (Figures 2b and S4). Both of the largest waves featured evident bore fronts and impacted the coast from significantly different directions; first from the northeast and then from the northwest (Figures 2a and S4). Although no CCTV cameras recorded the exact tsunami arrival time at Palu city, the panic on the scene observed at the beginning of videos 15 and 16 strongly suggests that the leading, smaller waves likely arrived less than 2 min after the earthquake. Because the first and second large trailing waves impacted 2 and 4 min after these initial inundations, respectively, the western sector of Palu city was likely devastated within 4-6 min of the mainshock, which is consistent with precise video observations at KN Hotel, Wani, and Pantoloan. Interestingly, if a single tsunami source is considered, the time span between waves at Palu city is consistent with a wave train period of ~2 min, which is unusually short for typical tectonic tsunamis (eg., Ward, 2011). Alternatively, the tsunamis that hit Palu city may have been caused by different sources, as suggested by their contrasting incoming directions.

Tsunami wavefronts impacting the local coastline with different orientations were apparently a hallmark of the Palu event, possibly produced by refraction in the shoaling of the waves due to the coastal bathymetry and/or by non-tectonic sources occurring close to the coast where observations were made. For instance, westward, coast-parallel inundation was captured by amateur videos in the eastern sectors of Palu city (videos 22 and 23). The KN Hotel CCTV footage simultaneously captured both eastward (videos 3 and 6) and westward (videos 1 and 2) inundations (Figure S1 and video 42). Unfortunately, the inundation at KN Hotel was nearly perpendicular to the evacuation road (video 6). This, combined with the nearly instantaneous arrivals (~100 s), prevented a successful evacuation (Figure S1). On the other hand, the fortunate orientation of the road perpendicular to the coastline near the Wani house allowed timely self-evacuations even from rapid tsunami arrivals (see Text S3). Vertical evacuation proved to be critical in areas where there was insufficient time available to evacuate horizontally, as revealed by video footage at the KN Hotel (video 4), eastern (videos 23 and 25–27), and western Palu (videos 1 and 5). The video analysis highlights the importance of addressing the possible directions of tsunami inundation in hazard assessments and their mitigation in planning evacuation routes, including vertical platforms if necessary, to reduce loss of life.

Overall, our video-based observations are consistent with high-amplitude tsunamis with sources near the coast (short arrival times), with unusually short periods (~2 min) and consequently short wavelengths. These tsunami characteristics resulted in rather high destructive capacity but limited capacity to inundate far inland (Satake et al., 2013). These characteristics are consistent with inland inundation distances inferred from satellite imagery (Figure S5), which provide a regional-scale assessment. Our interpretation of highresolution satellite images collected 3 to 4 days after the event (Digital Globe, 2018) suggests that severe devastation was confined to at most ~400 m inland (Figure S5). These characteristics are also consistent with the time-frequency signature of the Pantoloan tide gauge record, which shows that most of the initial energy was limited to 2- to 6-min periods (Figure S6). However, we note that the 1-min sampling interval of the Pantoloan record, which would usually be sufficient for characterizing subduction zone tsunamis, may be too coarse for capturing the tsunami patterns inferred from CCTV footage collected in the vicinity of the tide gauge station (video 11 and Figure S3). The vertical movements of the berthed container ship at Pantoloan port observed in video 11 are best explained by two tsunami waves (two troughs and two crests) occurring within less than 5 min after seismic shaking stopped (Figure S3). Interestingly, these waves were not captured by the local tide gauge station, which recorded longer-period fluctuations (~6 min) beginning with a leading drawdown at ~5 min following the mainshock (Figures 1c, 2b, and S6). Hence, our observations suggest that the Palu tsunamis included wave periods too short (~1-2 min) to be well captured by tide gauge running at the typical sampling intervals of 1 min. Whether the sea level fluctuations (periods of ~6 min) captured by the Pantoloan tide gauge have a different origin than the shorter-period waves observed in video footage, for example, from a combination of landslide and tectonic sources, or simply reflect an aliased version of shorter-period tsunami waves cannot be confirmed.



3. The Role of Coastal Landslides in the Palu Tsunamis

Our simulated tsunamis based on initial conditions from the fault slip models published to date (ie., Socquet et al., 2019; USGS, 2018) fail to fully explain the surveyed runups (Fritz et al., 2018) and cannot predict the tsunami waveforms inferred from our analysis of video footage (Figure 2; see methods for tsunami modeling). Aside from Dupa, where both slip models predict the video observations reasonably well, the inferred phases and amplitudes at the other five sites cannot be reproduced from these slip models (Figure 2b). This may be explained with three scenarios: (1) Slip models fail to predict the actual seafloor displacements beneath Palu Bay, which is possible owing to data limitations and uncertainties in both offshore fault geometry and seafloor mechanical properties; (2) our tsunami models fail to reproduce particular aspects of unusually short-period waves; and/or (3) additional nontectonic sources, such as submarine landslides triggered by strong seismic shaking (Bao et al., 2019), contributed to tsunami generation.

Widespread onshore landslides were triggered by the Palu earthquake (Petley, 2018; Sassa & Takagawa, 2019), and submarine slope failures may be a plausible mechanism to explain the additional sources required by the reconstructed tsunami waveforms. Indeed, the tsunamis observed in the tide gauge record at Mamuju, located ~200 km south of the Palu Bay (Figures 1a and 1c), may have been very likely triggered by landslides outside the bay. There, the local tide gauge station recorded tsunami amplitudes of up to 6 cm arriving 25 min after the mainshock. Based on simulated tsunami travel times, the source must be within 100 km of Mamuju, and thus is incompatible with the timing of a source near Palu Bay and the fault rupture (Figure 1a). Heidarzadeh et al. (2019) ascribed the Mamuju tsunami to the earthquake by proposing a 45-min delay on the tide gauge station clock to fit modeled and predicted waveforms; however, this assessment seems unlikely for two reasons. First, the official cancellation of the tsunami alert, 34 min after the earthquake, was decided based on the 6-cm small tsunamis recorded by the Mamuju tide gauge station (Hoffmann et al., 2018). And second, such a clock error would also imply a delay between the tides of Mamuju and Pantoloan (Figure S7), which does not seem to be the case (Informasi Geospasial, 2018b). Therefore, shaking-triggered landslides are the most reasonable source for the tsunamis observed at Mamuju, which is interesting since seismic shaking in this area (enclosed by the 25-min isoline in Figure 1a) is expected to be significantly less intense than in the area surrounding the fault zone, especially within Palu Bay.

To explore the possible role of submarine landslides as tsunami sources within Palu Bay, we analyzed video footage and satellite images to determine likely source regions. A detailed comparison of pre-and post-earth-quake satellite imagery revealed evidence of shoreline retreat at 18 sites around Palu Bay of distances from 10 to 120 m (Figures 2 and S8). Interestingly, all cases occurred along coastal plains adjacent to fluvial and alluvial fan deltas (Figure S8) and, therefore, may be interpreted as the surface expressions of submarine failures of these landforms. Deltas, formed from unconsolidated material, are very sensitive to failure by an external trigger such as seismic shaking (Girardclos et al., 2007; Hasiotis et al., 2006; Hilbe & Anselmetti, 2014; Leithold et al., 2018). Furthermore, the potential for delta failures to generate significant tsunamis during strong shaking events (Vanneste et al., 2018) has been documented at sites with diverse climatic conditions, such as Alaska (USA; Field et al., 1982; Parsons et al., 2014) and Haiti (Hornbach et al., 2010).

Evidence for tsunamis induced by delta failures during the Palu event is supported by video footage. Four extraordinary amateur videos, taken from a plane, a moored boat and from high ground captured the initiation and/or early formation of 7 tsunamis along the west coast of the bay (Figure 3 and videos 38–41). Strikingly, all of these came from areas where delta landforms failed during the Palu earthquake (Figures 2a and S8). However, based on their small sizes and late timing, they seem unlikely to be the complementary sources required to explain all the tsunami observations around Palu Bay. In order to explore whether similar sources occurred elsewhere in the bay, we interviewed Ricoseta Mafella, the aircraft pilot who collected video 38. Although he noticed that these sea level phenomena were only present along the western coast of the bay, he only had a clear view of the eastern flank about 3 min after the mainshock when he turned "left" (west). This time, however, may be too late given the nearly instantaneous occurrence of the Palu tsunamis and therefore, tsunamis triggered by submarine landslides along the eastern shore of the bay cannot be ruled out. Indeed, a video recorded at Taipa (Figure 2a) captured a large tsunami wave coming from the northeast coast of the bay (video 31 and Figures 3e and 3h). Although not as evident as the landslide tsunamis originating along the west coast, the steepness and seaward traveling direction of the wave seen in

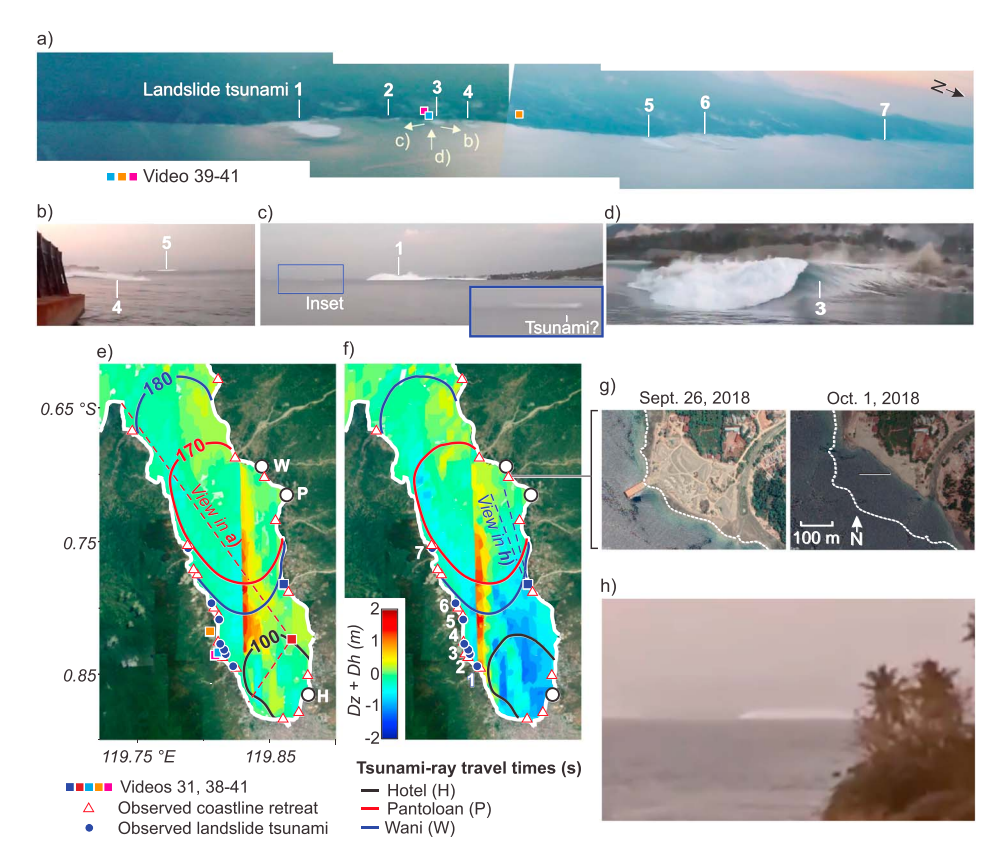


Figure 3. Examples of tsunamis interpreted to have been associated with submarine landslides and probable landslide locations inferred from a combined analysis of pre-and post earthquake satellite imagery and video footage. (a) Seven point-source sea level perturbations along the western coast of Palu Bay captured at ~1,000-m elevation by aircraft pilot Ricosseta Mafella (video 38). In the vicinity of landslide tsunami 3, a boat captured the tsunamis shown in (b)–(d) (video 39). Inset in (c) shows an additional sea level perturbation which could have been the first large wave to hit Palu (see text). (e) and (f) Tsunami-ray travel times (in seconds) from Wani, Pantoloan, and KN Hotel superimposed on vertical displacements of the sea surface due to vertical coseismic deformation (Dz) and the bathymetry effect (Dh; Tanioka & Satake, 1996), predicted by the fault slip models (Socquet et al., 2019; USGS, 2018, respectively). (g) Pre-and post-earthquake satellite images showing the shoreline between Pantoloan and Wani. Note pronounced retreat of the deltaic coastal plain. (h) Snapshot of video 31 when filming toward the north of the bay where a tsunami wave propagates seaward (see video 31).

the video seem more consistent with a localized source near the coastline than one produced by the earthquake faulting beneath the bay.

The precise arrival times estimated at Wani, Pantoloan, and the KN Hotel can be used to locate probable individual landslides sources. Figures 3e and 3f show the possible source regions predicted from backward tsunami-ray tracing from the video-inferred arrival times (methods), superimposed on the seafloor displacement patterns predicted by rupture models (Socquet et al., 2019; USGS, 2018) and coastline retreats inferred by satellite imagery (Figure S8). These isolines cross the areas of largest seafloor displacement and include multiple locations of coastline retreat, suggesting that the rapid arrival times at these three locations can be explained either by fault slip or by delta failures associated with such coastline retreats. However, the tsunami amplitudes reconstructed at these locations are 3 times greater than those predicted by tsunami simulations based on seafloor displacements (Figure 2b), and therefore, fault slip alone fails to fully explain the video-observed tsunamis at Wani, Pantoloan, and KN Hotel. Although bathymetric surveys are needed to address the occurrence of delta failures near the locations of coastline retreat, they are plausible candidates for localized, complementary tsunami sources. Particularly intriguing is the region between Pantoloan and Wani (Figure 3g), where we mapped the largest coastline retreat in Palu Bay (up to ~120 m). Failure of a delta front there would produce an immediate sea level drawdown followed by rapid tsunami inundation, as has been predicted by numerical simulations of other tsunamis (Watts et al., 2005) and reported by eyewitnesses to the tsunamis produced by delta



failures triggered by the 2010 Haiti earthquake (Hornbach et al., 2010). Interestingly, such a sea level response was inferred from video footage and eyewitness reports immediately north (Wani) and south (Pantoloan) of this pronounced coastline retreat (Text S2 and S3 and video 11). Although plausible, whether or not this was the source for the large wave propagating seaward from this part of the bay (Figures 3e and 3h), as seen in video 31, cannot be confirmed with the available data.

4. Concluding Remarks and Future Work

Our video-based analysis indicates that although the Palu earthquake was produced by predominantly horizontal fault slip, it generated devastating tsunamis reaching widespread coastal areas of Palu Bay nearly instantaneously, within tens of seconds after the end of seismic shaking. Shallow slip extending to the surface combined with the steep bathymetry of the long and narrow Palu Bay likely contributed to the large runups observed around the bay, which were further enhanced by the high tide (~1 m above MSL) at the time of the tsunami (Figure 1b). However, we note that tsunami simulations from existing fault slip models are not sufficient to reproduce the runup heights measured in field surveys, and cannot explain the spatial and temporal patterns inferred from the video-derived tsunami waveforms and local tide gauges. Unless these fault models underestimate the actual dip-slip component beneath Palu Bay, additional non-tectonic tsunami sources are likely to have contributed to tsunami generation. In this case, submarine landslides triggered by delta failures along the bay are plausible candidates for such supplementary sources, as suggested by locations of observed coastline retreat, video footage and tsunami-ray travel time simulations.

Our results provide valuable data and guidance for future efforts aimed at understanding the sources of the Palu tsunamis. Our inferred tsunami waveforms (available in the supporting information) may be used to test future fault slip models with improved offshore resolution and guide dedicated modeling experiments of tsunamis generated by a combination of submarine landslides and coseismic seafloor deformation. Additionally, our satellite imagery results can guide detailed bathymetric surveys where delta failures, potentially acting as tsunami sources, may have occurred. Based on our video analysis, we emphasize that future studies should use tsunami modeling strategies capable of simulating the generation, propagation and runup of unusually short-period tsunamis such as those observed. Finally, we highlight that the 1-min sampling interval of the Pantoloan tide gauge record did not reliably capture the damaging short-period features of the Palu tsunamis inferred from our analysis of CCTV footage captured in the vicinity of the station. This instrumental limitation, revealed by our analysis of video footage, has critical implications for tsunami early warning systems based on real-time sea level observations along coasts adjacent to diverse tectonic settings.

The tragic Palu story highlights several important lessons to be considered in areas with similar geomorphic and tectonic settings potentially exposed to tsunami hazards. The main lesson is that tsunami risk needs to be assessed locally; hazard assessments must consider all reasonable sources of tsunami generation based on the local tectonic setting and including areas of potential landslides. Also, because inundation and damage caused by short period waves can be quite different than those caused by longer period waves in a limited coastal inundation zone, a locally defined spectrum of wave periods must be considered, and according modeling strategies and bathymetric data must be used. Local infrastructure and urban design should consider this and other local aspects of tsunami hazards. The Palu tsunamis demonstrated that damaging waves may arrive within a few minutes after the seismic shaking, and therefore, escape routes must be appropriately located and oriented to allow timely self-evacuations, and if not possible, vertical evacuation shelters must be implemented.

Our waveform reconstructions from video footage complement previous video-based approaches (e.g., Fritz et al., 2006, 2012; Koshimura & Hayashi, 2012) aimed to better understand tsunami phenomena. We encourage the increased scientific use of tsunami videos shared on social media platforms that provide valuable constraints for scientific studies and help guide tsunami hazard mitigation efforts and focused post-tsunami surveys.

References

Associated Press (2018). Indonesia Earthquake Ship. http://www.aparchive.com/metadata/youtube/abf7ff674bfc102aec5cdf7b7a959423
Bao, H., Ampuero, J. P., Meng, L., Fielding, E. J., Liang, C., Milliner, C. W., et al. (2019). Early and persistent supershear rupture of the 2018 magnitude 7.5 Palu earthquake. *Nature Geoscience*, 12, 200–205. https://doi.org/10.1038/s41561-018-0297-z

Acknowledgments

This study is dedicated to all those who suffered in the 2018 Palu disaster. We deeply thank the aircraft pilot Ricoseta Mafella for kindly providing useful information about the aerial video (video 29) and those who shared their sad experience in YouTube. We also thank Patricio Winckler, Jasper Moernaut, Matt Miller, Manuel Contreras, and Maarten Van Daele for fruitful discussions in the initial phases of this study and Anne Socquet for providing us the slip distribution data. This manuscript greatly benefited from the comments of two anonymous reviewers. Funding came from the Iniciativa Científica Milenio (ICM) through Grant NC160025 "Millennium Nucleus CYCLO: The Seismic Cycle Along Subduction Zones." and by Chile's Fondo Nacional de Desarrollo Científico y Tecnológico, FONDECYT Project 1190258. I. S. acknowledges the support of the Miles Postdoctoral Fellowship by the Green Foundation. Data Set S1, which provides all the videos used here, is available at the website (https://agsweb.ucsd.edu/ tsunami/2018-09-28_palu/). The digital waveforms reconstructed from video footage are available in Data Set S2.



- Bellier, O., Sébrier, M., Beaudouin, T., Villeneuve, M., Braucher, R., Bourlès, D., et al. (2001). High slip rate for a low seismicity along the Palu-Koro active fault in central Sulawesi (Indonesia). *Terra Nova*, 13, 463–470. https://doi.org/10.1046/j.1365-3121.2001.00382.x
- Chicago Tribune (2018). Crew members recount terror of tsunami that dumped 208-foot ferry in Indonesian village. https://www.chicagotribune.com/news/nationworld/ct-indonesia-tsunami-ferry-ashore-20181004-story.html
- Cienfuegos, R., Catalán, P. A., Urrutia, A., Benavente, R., Aránguiz, R., & González, G. (2018). What can we do to forecast tsunami hazards in the near field given large epistemic uncertainty in rapid seismic source inversions? *Geophysical Research Letters*, 45, 4944–4955. https://doi.org/10.1029/2018GL076998
- Digital Globe (2018). Open Data program, Indonesia earthquake and Tsunami. https://www.digitalglobe.com/opendata/indonesia-earthquake-tsunami/post-event
- Field, M. E., Gardner, J. V., Jennings, A. E., & Edwards, B. D. (1982). Earthquake-induced sediment failures on a 0.25° slope, Klamath River delta, California. *Geology*, 10(10), 542–546. https://doi.org/10.1130/0091-7613(1982)10<542:ESFOAS>2.0.CO;2
- Fritz, H. M., Borrero, J. C., Synolakis, C. E., & Yoo, J. (2006). 2004 Indian Ocean tsunami flow velocity measurements from survivor videos. Geophysical Research Letters, 33, L24605. https://doi.org/10.1029/2006GL026784
- Fritz, H. M., Phillips, D. A., Okayasu, A., Shimozono, T., Liu, H., Mohammed, F., et al. (2012). The 2011 Japan tsunami current velocity measurements from survivor videos at Kesennuma Bay using LiDAR. *Geophysical Research Letters*, 39, L00G23. https://doi.org/10.1029/2011GL050686
- Fritz, H. M., Synolakis, C., Kalligeris, N., Skanavis, V., Santoso, F., Rizal, M., et al. (2018). Field survey of the 28 September 2018 Sulawesi tsunami. Eos, Transactions of the American Geophysical Union, 99, 53.
- Girardclos, S., Schmidt, O. T., Sturm, M., Ariztegui, D., Pugin, A., & Anselmetti, F. S. (2007). The 1996 AD delta collapse and large turbidite in Lake Brienz. *Marine Geology*, 241(1-4), 137–154. https://doi.org/10.1016/j.margeo.2007.03.011
- Hasiotis, T., Charalampakis, M., Stefatos, A., Papatheodorou, G., & Ferentinos, G. (2006). Fan delta development and processes offshore a seasonal river in a seismically active region, NW Gulf of Corinth. *Geo-Marine Letters*, 26(4), 199–211. https://doi.org/10.1007/s00367-006-0020-8
- Heidarzadeh, M., Muhari, A., & Wijanarto, A. B. (2019). Insights on the source of the 28 September 2018 Sulawesi tsunami, Indonesia based on spectral analyses and numerical simulations. *Pure and Applied Geophysics*, 176(1), 25–43. https://doi.org/10.1007/s00024-018-2065-9 Hilbe, M., & Anselmetti, F. S. (2014). Signatures of slope failures and river-delta collapses in a perialpine lake (Lake Lucerne, Switzerland).
- Sedimentology, 61(7), 1883–1907. https://doi.org/10.1111/sed.12120
- Hoffmann T., Triyono R., Weniza, A., Heryandoko, N., Daniarsyad, G., Karyono, A., et al. (2018). The 2018 Mw 7.5 Sulawesi Indonesia earthquake: The immediate response of the InaTEWS Warning Centre at BMKG and related operational issues. Paper presented at the Fall Meeting, AGU, Washington DC, December 10-14, 2018.
- Hornbach, M. J., Braudy, N., Briggs, R. W., Cormier, M.-H., Davis, M. B., Diebold, J. B., et al. (2010). High tsunami frequency as a result of combined strike-slip faulting and coastal landslides. *Nature Geoscience*, 3(11), 783. https://doi.org/10.1038/ngeo975
- Imamura, F., Synolakis, C. E., Gica, E., Titov, V., Listanco, E., & Lee, H. J. (1995). Field survey of the 1994 Mindoro Island, Philippines tsunami. *Pure and Applied Geophysics*, 144(3-4), 875–890. https://doi.org/10.1007/BF00874399
- Informasi Geospasial (2018a). Contour map of Palu Bay, Retrieved from https://cloud.big.go.id. Accessed 15 Oct. 2018.
- Informasi Geospasial (2018b). Real time tidal observation, Retrieved from http://tides.big.go.id:8888/dash/. Accessed 28 Feb. 2019.
- Katili, J. A. (1970). Large transcurrent faults in Southeast Asia with special reference to Indonesia. *Geologische Rundschau*, 59(2), 581–600. https://doi.org/10.1007/BF01823809
- Koshimura, S., & Hayashi, S. (2012). Tsunami flow measurement using the video recorded during the 2011 Tohoku tsunami attack. In 2012 IEEE International Geoscience and Remote Sensing Symposium (pp. 6693–6696). Munich, Germany: IEEE. https://doi.org/ 10.1109/IGARSS.2012.6352063
- Leithold, E. L., Wegmann, K. W., Bohnenstiehl, D. R., Smith, S. G., Noren, A., & O'Grady, R. (2018). Slope failures within and upstream of Lake Quinault, Washington, as uneven responses to Holocene earthquakes along the Cascadia subduction zone. *Quaternary Research*, 89(1), 178–200. https://doi.org/10.1017/qua.2017.96
- Mori, N., Takahashi, T., Yasuda, T., & Yanagisawa, H. (2011). Survey of 2011 Tohoku earthquake tsunami inundation and run-up. Geophysical Research Letters, 38, L00G14. https://doi.org/10.1029/2011GL049210
- Muhari, A., Imamura, F., Arikawa, T., Hakim, A. R., & Afriyanto, B. (2018). Solving the puzzle of the September 2018 pale, Indonesia, tsunami mystery: Clues from the tsunami waveform and the initial field survey data. *Journal of Disaster Research*, 13, sc20181108.
- Omira, R., Dogan, G. G., Hidayat, R., Husrin, S., Prasetya, G., Annunziato, A., et al. (2019). The September 28th, 2018, tsunami in Palu-Sulawesi, Indonesia: A post-event field survey. *Pure and Applied Geophysics*, 1–17.
- Parsons, T., Geist, E. L., Ryan, H. F., Lee, H. J., Haeussler, P. J., Lynett, P., et al. (2014). Source and progression of a submarine landslide and tsunami: The 1964 Great Alaska earthquake at Valdez. *Journal of Geophysical Research: Solid Earth*, 119, 8502–8516. https://doi.org/10.1002/2014JB011514
- Petley, D. (2018). Landslide tsunamis from the Sulawesi earthquake. The Landslide Blog, 19 October 2018. https://blogs.agu.org/landslideblog/2018/10/19/landslide-tsunamis-sulawesi-earthquake
- Prasetya, G. S., De Lange, W. P., & Healy, T. R. (2001). The Makassar Strait tsunamigenic region, Indonesia. *Natural Hazards*, 24(3), 295–307. https://doi.org/10.1023/A:1012297413280
- Sassa, S., & Takagawa, T. (2019). Liquefied gravity flow-induced tsunami: First evidence and comparison from the 2018 Indonesia Sulawesi earthquake and tsunami disasters. *Landslides*, 16(1), 195–200. https://doi.org/10.1007/s10346-018-1114-x
- Satake, K., Fujii, Y., Harada, T., & Namegaya, Y. (2013). Time and space distribution of coseismic slip of the 2011 Tohoku earthquake as inferred from tsunami waveform data. *Bulletin of the Seismological Society of America*, 103(2B), 1473–1492. https://doi.org/10.1785/0120120122
- Socquet, A., Hollingsworth, J., Pathier, E., & Bouchon, M. (2019). Evidence of supershear during the 2018 magnitude 7.5 Palu earthquake from space geodesy. *Nature Geoscience*, 12(3), 192–199. https://doi.org/10.1038/s41561-018-0296-0
- Socquet, A., Simons, W., Vigny, C., McCaffrey, R., Subarya, C., Sarsito, D., et al. (2006). Microblock rotations and fault coupling in SE Asia triple junction (Sulawesi, Indonesia) from GPS and earthquake slip vector data. *Journal of Geophysical Research*, 111, B08409. https://doi.org/10.1029/2005JB003963
- Soloviev, S. L., & Go, C. N. (1974). A Catalogue of Tsunamis on the Western Shore of the Pacific Ocean. Moscow: Nauka Publishing House. Tanioka, Y., & Satake, K. (1996). Tsunami generation by horizontal displacement of ocean bottom. Geophysical Research Letters, 23(8), 861–864. https://doi.org/10.1029/96GL00736
- U.S. Geological Survey (2018). M 7.5-70km N of Palu, Indonesia, https://earthquake.usgs.gov/earthquakes/eventpage/us1000h3p4/finite-fault



- Vanneste, K., Wils, K., & Van Daele, M. (2018). Probabilistic evaluation of fault sources based on paleoseismic evidence from mass-transport deposits: the example of Aysén Fjord, Chile. *Journal of Geophysical Research: Solid Earth*, 123, 9842–9865. https://doi.org/10.1029/2018JB016289
- Walpersdorf, A., Vigny, C., Manurung, P., Subarya, C., & Sutisna, S. (1998). Determining the Sula block kinematics in the triple junction area in Indonesia by GPS. *Geophysical Journal International*, 135(2), 351–361. https://doi.org/10.1046/j.1365-246X.1998.00641.x
- Ward, S. (2011). Tsunami. In H. K. Gupta (Ed.), Encyclopedia of Solid Earth Geophysics, Encyclopedia of Earth Sciences Series (pp. 1473–1493). Dordrecht: Springer. https://doi.org/10.1007/978-90-481-8702-7
- Watkinson, I. M., & Hall, R. (2017). Fault systems of the eastern Indonesian triple junction: evaluation of Quaternary activity and implications for seismic hazards. Geological Society, London, Special Publications, 441(1), 71–120. https://doi.org/10.1144/SP441.8
- Watkinson, I. M., Hall, R., Cottam, M. A., Sevastjanova, I., Suggate, S., Gunawan, I., et al. (2012). New insights into the geological evolution of Eastern Indonesia from recent research projects by the SE Asia Research Group. *Berita Sedimentologi*, 23, 21–27.
- Watts, P., Grilli, S. T., Tappin, D. R., & Fryer, G. J. (2005). Tsunami generation by submarine mass failure. II: Predictive equations and case studies. *Journal of Waterway, Port, Coastal, and Ocean Engineering*, 131(6), 298–310.

References From the Supporting Information

- Okada, Y. (1985). Surface deformation due to shear and tensile faults in a half-space. Bulletin of the Seismological Society of America, 75(4), 1135–1154.
- Pawlowicz, R., Beardsley, B., & Lentz, S. (2002). Classical tidal harmonic analysis including error estimates in MATLAB using T_TIDE. Computers & Geosciences, 28(8), 929–937. https://doi.org/10.1016/S0098-3004(02)00013-4
- Torrence, C., & Compo, G. P. (1998). A practical guide to wavelet analysis. *Bulletin of the American Meteorological Society*, 79(1), 61–78. https://doi.org/10.1175/1520-0477(1998)079<0061:APGTWA>2.0.CO;2
- Wang, X. (2009). User manual for COMCOT version 1.7 (first draft). Cornel University, 65.